Electrochemically enhanced simultaneous degradation of sulfamethoxazole, ciprofloxacin and amoxicillin from aqueous solution by multi-walled carbon nanotube filter

Ting-Yuan Tan[a,1], Zhuo-Tong Zeng[b,1], Guang-Ming Zeng[a,*], Ji-Lai Gong[a,*], Rong Xiao[b,*], Peng Zhang[a], Biao Song[a], Wang-Wang Tang[a], Xiao-Ya Ren[a]

[a] College of Environmental Science and Engineering, Hunan University and Key Laboratory of Environmental Biology and Pollution Control (Hunan University), Ministry of Education, Changsha 410082, PR China
[b] Department of Dermatology, Second Xiangya Hospital, Central South University, Changsha 410011, PR China

ARTICLE INFO

ABSTRACT

Electrochemical filters exhibited excellent properties of time saving and energy conservation and were widely used in water purification. In this work, an efficient method was proposed for degrading antibiotics including sulfamethoxazole (SMZ), ciprofloxacin (CIP) and amoxicillin (AMO) in both single system and mixed system by utilizing multi-walled carbon nanotube (MWCNT)-based electrochemical membrane. The effect of experimental parameters was investigated with respect to voltage, pH, temperature, initial pollutant concentration and sodium dodecyl benzene sulfonate (SDBS). The recycling experiments of MWCNT-based electrochemical filter were also performed. Results revealed that the degradation efficiency could be enhanced by increasing the voltage and temperature, while it decreased with the increased initial pollutant concentration and the addition of SDBS. Degradation of SMZ and AMO was weakly affected by solution pH. However, the degradation efficiency of CIP in acidic or alkaline solution was much higher than that in neutral solution. Furthermore, the MWCNT-based electrochemical membrane still exhibited high efficiency for antibiotic degradation after reuse of four times, which could facilitate the development of reproducible and low-cost pollutant-processing method. Noticeably, this membrane filter also presented high performance on simultaneously removing the multiple antibiotics with the efficiency order of AMO (98%) > SMZ (95%) > CIP (20%). The degradation mechanism of antibiotics by the MWCNT-based membrane was analyzed and a clear explanation on the antibiotics-removed pathway was provided. These results indicated that the MWCNT-based electrochemical membrane filtration may have potential to effectively treat multiple antibiotics in real wastewater.

1. Introduction

Much effort are being made for purifying the waste water due to the massive industry-discharged inorganic/organic pollutants such as, chemicals, dyes, drugs and pesticides [1-3]. Due to the characteristics of complex structure, high strength, hard degradation, and high activity of their metabolites, antibiotic drugs released to aqueous environment inevitably cause water pollution [4,5]. Therefore, antibiotics have put some challenges for waste water treatment, thus posing potential hazards to environment and health [6]. The types and concentrations of antibiotics in the aquatic environment are not the same for different countries and modes of use. Europe presents a north-south gradient, with usage in the north (Finland, Slovakia, etc.) significantly lower than

in the south (Italy, Spain, etc.) [7]. However, there are significant east-west differences in China, with the average emission density of antibiotics in the eastern cities being 6 times that of the western cities [8]. According to reports, in 2013, the ratio of sulfonamides, quinolones and β-lactam antibiotics in Europe was 2.9%, 8.3% and 11.3%, respectively. However, their ratios in China are 5%, 17% and 21%, respectively [7,8]. Globally, the detection range of antibiotics has reached from ppm to ppt levels, even after the wastewater treatment plants (WWTPs). In Europe, including Croatia, Germany and Portugal, the concentration of sulfonamides after WWTPs was approximately 2 μg/l [7]. In Asia, quinolones and sulfonamides were found after WWTP in Beijing, with an average concentration of 5 and 3 μg/L, respectively [9]. In South Korea, tetracycline and sulfonamides after WWTP are also at ppb levels [10].

However, it is well known that organisms in the environment are generally not exposed to a single compound but are exposed to a mixture of antibiotics [11]. Leung et al. reported that 89% of 113 samples of tap water in 13 Chinese cities contained 17 drugs [12]. Therefore, it is necessary and urgent to simultaneously remove multiple antibiotics and their conversion products.

Traditional methods for removing antibiotics in water include coagulation, adsorption, and biological systems. They have certain limitations. A disadvantage of these conventional processes is that they do not real degrade the contaminants but concentrate and transfer them to produce new waste that requires subsequent processing to remove the new waste [13,14]. Hence, various new technologies have been subsequently studied to degrade antibiotics. Advanced oxidation processes based on electrochemical technology have attracted more and more attention as an alternative for traditional methods [15-17].

Electrochemical oxidation refers to generating free radicals through a series of reactions in a certain container, such as solvated electron, $\cdot OH$, $\cdot O_2$, and $Cl\cdot$ on the anode. These free radicals can decompose pollutants and the process is irreversible. Usually this method is also seen as a greener alternative to other approaches [18]. Several electrode materials were tested for the degradation of amoxicillin (AMO), the study showed that BDD had proven to be the best anode material at high current densities, forming a large number of hydroxyl radicals and other oxidants such as hydrogen peroxide, which contributed to the enhancement of oxidation and mineralization of AMO [19]. Recently, ceramic electrodes based on sub-stoichiometric titanium oxides, particularly Ti_4O_7 was systematically studied for degradation and mineralization of AMO [20]. However, the strict conditions, not enough efficiency and high operating costs due to high energy consumption were still the main drawbacks limiting the large-scale application of electrochemical processes. For example, the antibiotic amoxicillin was completely mineralized with BDD anodic Fenton, but the pH requirement was strong acid [21]. Homem et al. summarized that direct oxidation efficiency depended on the catalytic activity of the electrode, the diffusion rate of the anode active compound and the current, while the indirect oxidation was strongly dependent on the diffusion rate of the oxidizing agent in the solution, the temperature and pH [13]. In the electrochemical cell amoxicillin elimination was only 80% after 240 min of degradation [22]. Therefore, it is an urgent need to further improve the degradation efficiency of antibiotics using new approaches.

Membrane filtration technologies were efficient ways of removing water micro-pollutants [23]. There have been some studies on the removal of micro-pollutants in water by carbon nanotube membranes. Wang et al. have studied the pre-coagulation of wastewater by filtration through carbon nanotube membranes to remove acetaminophen, triclosan, caffeine and carbendazim [24]. Hybrid carbon membrane also was studied to remove tetracycline antibiotics in water [25]. Nano-composite membranes containing single-walled and multi-walled carbon nanotubes (SWCNTs and MWCNTs) have been reported for the filtration of triclosan, acetaminophen and ibuprofen [26]. Acid-treated carbon nanotubes and Polyvinyl chloride (PVC) polymeric ultrafiltration membranes were also reported to remove bisphenol A and norfloxacin from drinking water [27]. Although membrane filtration has been used to remove more complex contaminants, it still was dependent on initial concentration, ionic strength, pH, membrane fouling and transmembrane pressure are challenges for membrane filtration [28].

Compared to conventional filtration systems, electro-catalytic membranes with higher removal efficiencies can provide the removal of the target pollutants by both adsorptive filtration and electrochemical degradation under applied voltage, thus avoiding time-consuming requirements and lowering energy consumption [29]. Carbon nanotubes (CNTs) were a new type of porous structure adsorbents with good electrical conductivity and strong interaction with contaminants [30]. There were some studies have summarized coupling of membrane filtration and advanced oxidation processes for removal of pollutants [31,32]. CNT-based electro-catalytic membranes with appropriate size

and configuration pores possessed three times higher performance than that of conventional polymeric electro-catalytic membranes without well-defined pores [33]. In addition, CNT-based electro-catalytic membranes exhibited stable, conductive and porous three-dimensional networks for enhanced ion and molecular transport [34]. Liu reported that main mechanism of electrochemical membrane filtration depended on mass transfer, physical adsorption and electron transfer [35]. Recently, it was reported that carbon nanotube based filters use electrochemical catalysis to degrade pollutants. The first discovered electrochemical MWCNT filter was used as a drinking water purification technology for pathogen removal and inactivation, whereby the application potential was developed [36]. A significant removal of bisphenol A with identical performance was also reported using both pristine and boron-doped MWNT-based filters [37]. Results showed that oxidation reaction dominates at a higher voltage (2–3 V) and surface adsorption played an important role under a lower voltage (0–1 V) [37]. Noticeably, CNT network cathode filter was developed to remove antibiotic tetracycline. Compared with perforated Ti cathode filter, CNT network filter is performed at a lower cell voltage to achieve similar performance, thus greatly reducing energy consumption [38]. Tetracycline was also degraded using a Nano-TiO_2/carbon electro-catalytic membrane. It was found that the removal efficiency for tetracycline was almost independent on pH value and tetracycline was completely removed at the concentration of 50 mg/L [39]. A conductive cellulose-based cotton electrochemical filter was documented by incorporating CNT as fillers to remove ferrocyanide, methyl orange and antibiotic tetracycline [40]. Moreover, results showed that the maximum electrooxidation flux was 0.9 mol/h/m^2 for 0.2 mmol/L tetracycline [40]. In the cross-flow filtration mode combined with electrochemical oxidation, the effects of permeate flux, contaminant concentration and current density on the mineralization efficiency of various organic compounds (oxalic acid, acetaminophen, phenol) were systematically evaluated [41]. The removal mechanism of p-nitrophenol, p-methoxyphenol and p-benzoquinone on the porous Ti_4O_7 reaction electrochemical membrane under anodic polarization was also investigated, which indicated that $\cdot OH$ was mainly formed by electrochemical reaction [42]. The perusal of the literature indicated that CNT-based electrochemical membrane filtration was applied for removing only single antibiotic in wastewater. No literature was reported on the application of electrochemical CNT-based membrane filtration to remove multiple antibiotics in wastewater.

In this study, an electrochemical membrane filter was fabricated using MWCNT as anode and perforated stainless steel as cathode for simultaneous removal of multiple antibiotics including sulfamethoxazole (SMZ), ciprofloxacin (CIP) and amoxicillin (AMO). We studied on the application of electrochemical CNT-based membrane filtration to degrade antibiotics in wastewater. And we systematically studied the simultaneously removal of multiple antibiotics. Background curve and breakthrough curves were completed to investigate electron transfer and sorption processes, respectively. Experimental factors that influence the degradation efficiency, such as voltage, pH, temperature, concentration, sodium dodecyl benzene sulfonate (SDBS), recyclability were investigated. Mixed pollution systems included binary mixture (i.e., SMZ + CIP, SMZ + AMO, CIP + AMO) and ternary mixture (i.e., SMZ + CIP + AMO). The electrochemical mechanism and the degradation products were also investigated.

2. Materials and methods

2.1. Chemicals and materials

Sodium chloride (purity $\geq$ 99.5%, NaCl) was purchased from Tianjin Fengchuan Chemical Reagent Technologies Co. Ltd. SMZ (purity $\geq$ 99%, $C_{10}H_{11}N_3O_3S$), CIP (purity $\geq$ 99%, $C_{17}H_{18}FN_3O_3$) and AMO (purity $\geq$ 99%, $C_{16}H_{19}N_3O_5S$) were obtained from Sigma-Aldrich. Porous MWCNTs (purity $\geq$ 95%, d = 750 nm and l = 10–20 μm) were
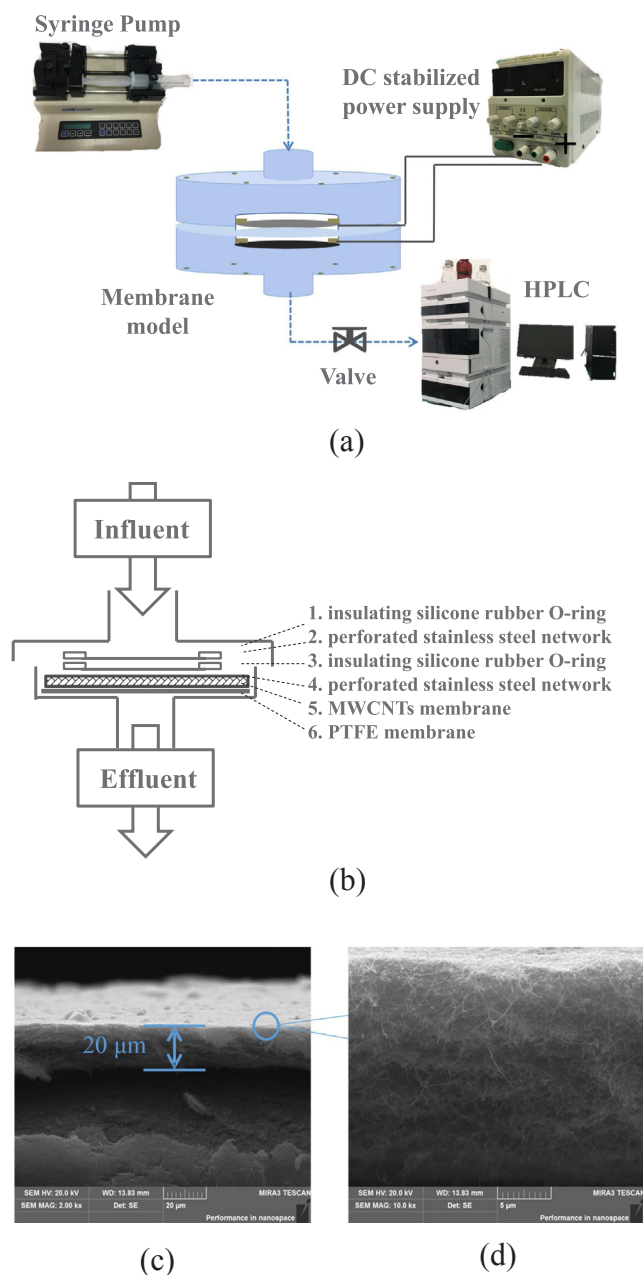
Fig. 1. (a) Diagram of the lab-scale electrical membrane filtration setup; (b) MWCNT electrochemical filter design and characterization; (c) the cross section SEM image of the anodic MWCNT filter membrane; (d) the SEM image of the MWCNTs.

purchased from Chengdu Organic Chemistry Co., Chinese Academy of Sciences, China. Ultrapure water (18.25 MΩ·cm, produced by Barnstead SMART2PURE system, ThermoFisher Scientific) was used throughout the whole experiments.

The MWCNT powders were dispersed in dimethyl formamide (DMF) and probe sonicating for 15 min (ultrasound time was 3 s, interval time was 4 s, power was 400 W). Then, the obtained MWCNT dispersion was filtered onto a 5 μm Poly tetra fluoroethylene (PTFE) membrane under vacuum condition. The MWCNT membrane was washed with 100 mL of ethanol, 250 mL of ultrapure water to remove DMF before use, resulting in filter loading area was 706 mm². NaCl was used as the background electrolyte (20 mM) to normalize ionic strength and conductivity, the influent concentration was 5 mg/L.

2.2. MWCNT electrochemical filtration setup

All filtration experiments were achieved using the improved electrochemical filtration casing as shown in Fig. 1a and b. A porous MWCNT network was put on a PTFE membrane (filtration area = 706 mm²) and laid into the improved electrochemical filtration casing. Cathode was composed of a stainless steel network. Anode was stainless steel network combined with porous MWCNT network which were coated on PTFE membrane. Insulating Si-rubber O-ring with 1 cm thickness was used to seal and separate the electrodes. In order to strengthen the conductivity, the anodic stainless steel network was put onto the MWCNT network. Typically, the influent flowed first through cathodic porous stainless steel networks, followed by anodic porous stainless steel networks, and finally an anodic MWCNT network and PTFE membrane.

2.3. Characterization

The Background curve was implemented to characterize electrochemical properties. A three-electrode system was used in this study including MWCNT working electrode, Ag/AgCl reference electrode, and a stainless steel wire counter electrode. This measurement was completed by an electrochemical workstation (CHI 660D, Shanghai Chenhua Instrument Co. Ltd., China). The surface morphology of the membrane was determined by scanning electron microscopy (SEM).

2.4. Breakthrough curve measurement

In the absence of a power source, a breakthrough curve experiment was performed. The influent concentration was 5 mg/L and effluent aliquots were collected every 3 min until the effluent concentration was equal to the influent concentration.

2.5. Evaluation of MWCNT electrochemical filtration performance

In this study, three different antibiotics including SMZ, CIP and AMO were chosen to evaluate the filtration performance of MWCNT electrochemical filtration membrane. The filtration experiments of different antibiotics were executed by a syringe filter. A syringe pumped ultrapure water at a speed of 1.5 mL/min to flush and calibrate the flow.

The effect of experimental parameters including antibiotic concentrations (i.e., 5 mg/L, 25 mg/L and 50 mg/L), voltages (i.e., 0 V, 1 V, 2 V and 3 V), pH values (3, 5, 7, 9 and 11) and temperatures (15 °C, 25 °C and 35 °C) were investigated. The effect of SDBS with a concentration of 5 mg/L on degradation efficiency was also investigated. MWCNT filter was washed by ethanol under vacuum condition after membrane filtration for further use.

Moreover, the mixed antibiotics solutions (i.e., binary system and ternary system) filtration experiments by MWCNT-based electrochemical membrane filtration were also performed at 25 °C. In the binary or ternary system, the concentration of each antibiotic was fixed at 5 mg/L. The total filtration volume was 100 mL. The effluent was collected every 5 min and analyzed by high performance liquid chromatography to confirm the target effluent concentration.

2.6. Analytical methods

The effluent was collected at given time intervals and its concentration was measured by an HPLC Series 1100 (Agilent, Waldbronn, Germany) equipped with a diode array detector (DAD). Noticeably, the effluent was first filtrated by 0.22 μm membrane filter with subsequent concentration analysis. The column was a C-18 column (4.6 × 250 mm) at the temperature of 40 °C. The mobile phase was a mixture of acetonitrile (A) and 0.1% v/v formic acid (B) at the flow rate 1 mL/min. Gradient elution was performed using 5% A and 95% B for 8.0 min,

followed by 15% A and 85% B for 12.0 min, and an equilibration time of 3 min and then back to initial value in 4 min. The sample volumes for injection were all 20 μL and the wavelength of detector was 275 nm (SMZ and CIP) and 228 nm (AMO). Under these conditions, the retention times of SMZ, CIP, and AMO were 4.3, 7.9 and 24.7 min, respectively.

A liquid chromatography mass spectrometry (LC–MS) (Agilent 1290/6460, Triple Quad MS, USA) was used to determine the intermediate products from SMZ, CIP and AMO degradations. For SMZ, the mobile phase was composed of acetonitrile (solvent A) and 0.1% formic acid dissolved in water (solvent B) in gradient flow. The elution program (mobile phase) for LC-MS analysis is as follows: from initial to 1 min, solvent A and B was used in the ratio of 10:90 (A:B = 10:90); from 2 min to 6 min, A:B = 40:60; from 7 min to 12 min, A:B = 60:40; from 13 min to 16 min, A:B = 80:20 and from 17 min to 20 min, A:B = 10:90, respectively. For CIP, the mobile phase composition was acetonitrile (A) and water containing 0.1% formic acid (B) at a flow rate of 0.25 mL/min. the mobile phase composition (A/B) started at 10/90 (v/v) with a linear increase to 90/10 (v/v) in 7 min, where it was held for 4 min. Then the gradient was returned to 10/90 (v/v) and kept for 5 min to allow for equilibration. For AMO, the mobile phase consisted of a mixture of solution A (0.1% formic acid in water) and solution B (0.1% formic acid in acetonitrile) with an initial composition of 90% solution A and 10% solution B. The mobile phase composition changed linearly from 10% solution B to 40% at 10.0 min, then solution B was re-equilibrated to starting conditions in 0.5 min and maintained for 1.5 min.

The mass spectrometer ionization source was operated in positive mode. The capillary and fragmentation voltages were 4000 and 100 V, respectively, the nebulizer pressure was 40 psi, and the temperature was 350 °C. The triple quadrupole mass spectrometer acquired data in multiple reactions monitoring mode.

3. Results and discussion

3.1. Electrochemical filter design and characterization

The schematic of the MWCNT-based electrochemical filter was presented in Fig. 1a and b. MWCNTs filter was operated anodically and was electrically connected via a perforated stainless steel wire. Another perforated stainless wire was connected to the DC power supply and was operated as the cathode. An insulating silicone rubber O-ring was used to separate the electrodes, and another insulating silicone rubber O-ring was used to densify this setup [43]. Fig. 1c presents the section of the MWCNT membrane, which was about 20 μm thick and exhibited stacked layers structure with an effective filtration area of 706 mm^2.

Current - Voltage (I - V) curves for sodium chloride electrolyte solutions can be found in Fig. 2 the change curves of the transient current with applied voltage and current in NaCl solution with different concentrations at a flow rate of 1.5 mL/min were drawn. At the same concentration, the current increased with increasing voltage. At all voltage conditions, as the concentration increased, the current also increased. When NaCl was added, the current increased linearly with the potential above 2.0 V. This is related to the one-electron oxidation of chlorine: $Cl^- + e^- \rightarrow Cl^·$ [43] (E° = 2.4 V). The NaCl concentration at 20 mmol/L was selected in the whole experiments.

3.2. Removal efficiencies of antibiotics using different methods

Both MWCNT-based adsorptive filtration and electrochemical degradation can remove antibiotics. Fig. 3 compares the breakthrough plots for the removal of SMZ (Fig. 3a), CIP (Fig. 3b), and AMO (Fig. 3c). The three kinds of antibiotics used three different methods including MWCNTs-based adsorptive filtration, electrochemical degradation without MWCNT membrane and MWCNT-based electrochemical membrane filtration. For SMZ, the adsorptive filtration efficiency was
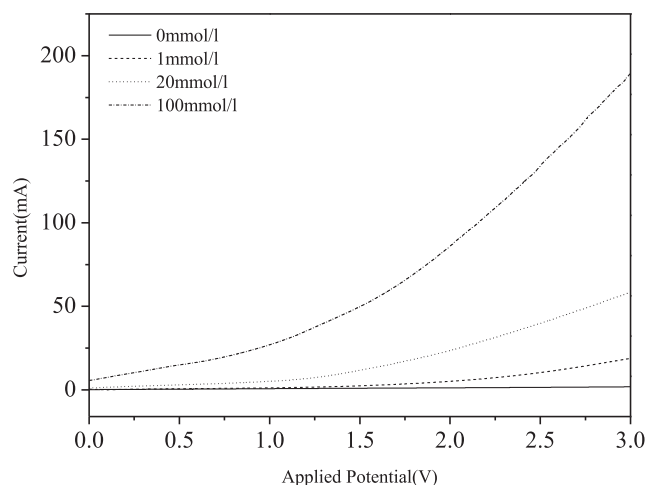
Fig. 2. Electrochemical MWCNT filter I-V curves as a function of NaCl concentration.

only 20% after 60 min, and electrochemical degradation efficiency was achieved at 75% after 60 min, while MWCNT-based electrochemical membrane filtration efficiency reached 90% after 60 min. At time < 12 min, the efficiency of MWCNT-based electrochemical membrane filtration was lower to the adsorptive filtration, suggesting that an electrostatic desorption occurred. Fig. 3b shows three kinds of removal efficiency for CIP. The adsorptive filtration efficiency was only 3% after 60 min, and electrochemical degradation efficiency was achieved at 60% after 60 min, while MWCNT-based electrochemical membrane filtration efficiency reached 76% after 60 min. At time < 18 min, the efficiency of MWCNT-based electrochemical membrane filtration was lower than the adsorptive filtration. At time < 28 min, the efficiency of MWCNT-based electrochemical membrane filtration was lower than electrochemical degradation, indicating that electrostatic desorption occurred when the voltage was applied. The results indicated that the absorption ability was suppressed when electric field was applied in a short time. Fig. 3c shows the adsorptive filtration efficiency for AMO was only 13% after 60 min, and electrochemical degradation efficiency was achieved at 94% after 60 min, while MWCNT-based electrochemical membrane filtration efficiency reached 98% after 60 min.

The physical sorption and the electrolysis were two major applied forces in the experiments, and the latter usually played a leading role [44]. When both physical sorption and the electrolysis simultaneously worked, the degradation efficiency of antibiotics was the best.

Fig. 4a shows the adsorption breakthrough curve, C_{eff}/C_{in} versus T, in the absence of electricity for three kinds of antibiotics. In all cases, the concentration of the antibiotics in the effluent was below the limitation of detection prior to breakthrough, indicating that all antibiotic molecules collided with the surface of the MWCNTs as they passed through the filter, causing them to be absorbed. The rapid adsorption can be attributed to its relatively strong van der Waals, $\pi - \pi$, and cation $- \pi$ interactions with the sp^2-conjugated MWCNTs [38]. Results showed that AMO was removed more quickly than SMZ and CIP. It also showed that the adsorption rate for AMO was higher than SMZ and CIP, and it was also much more exhausted than others. The absorption capacities for AMO, SMZ and CIP were 6.47, 5.52 and 1.49 mg/g, respectively. Due to the thin film properties of the filter, the total removal capacity of the MWCNT filter was relatively low compared to other membrane filtration (displayed in Table S1). As shown in Fig. 4b, AMO was the easiest to be electrolyzed, followed by SMZ and CIP. Noticeably, the removal efficiency for CIP was higher than SMZ at the time less than 30 min, nevertheless, the removal efficiency for CIP was lower than SMZ at the time more than 30 min owing to the different structures. According to Fig. 4c, after an hour of MWCNT-based electrochemical membrane filtration, AMO was almost completely degraded,
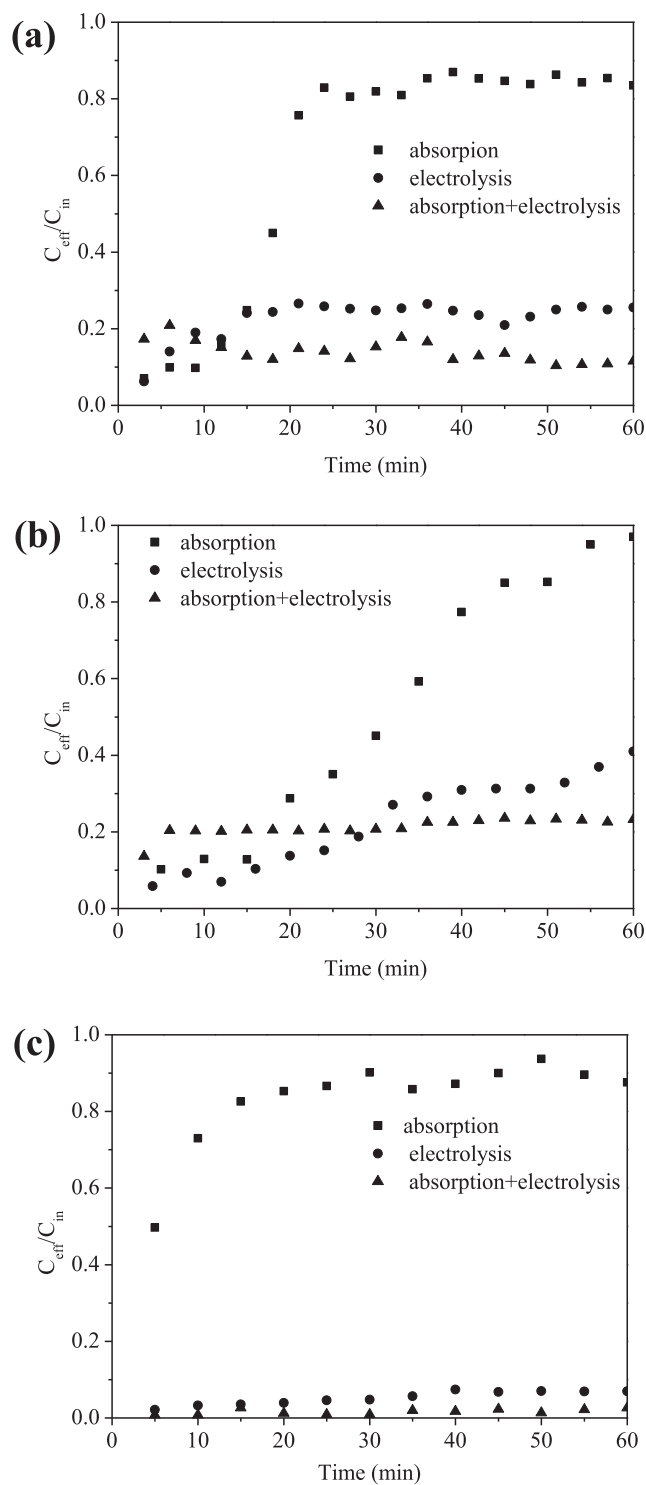
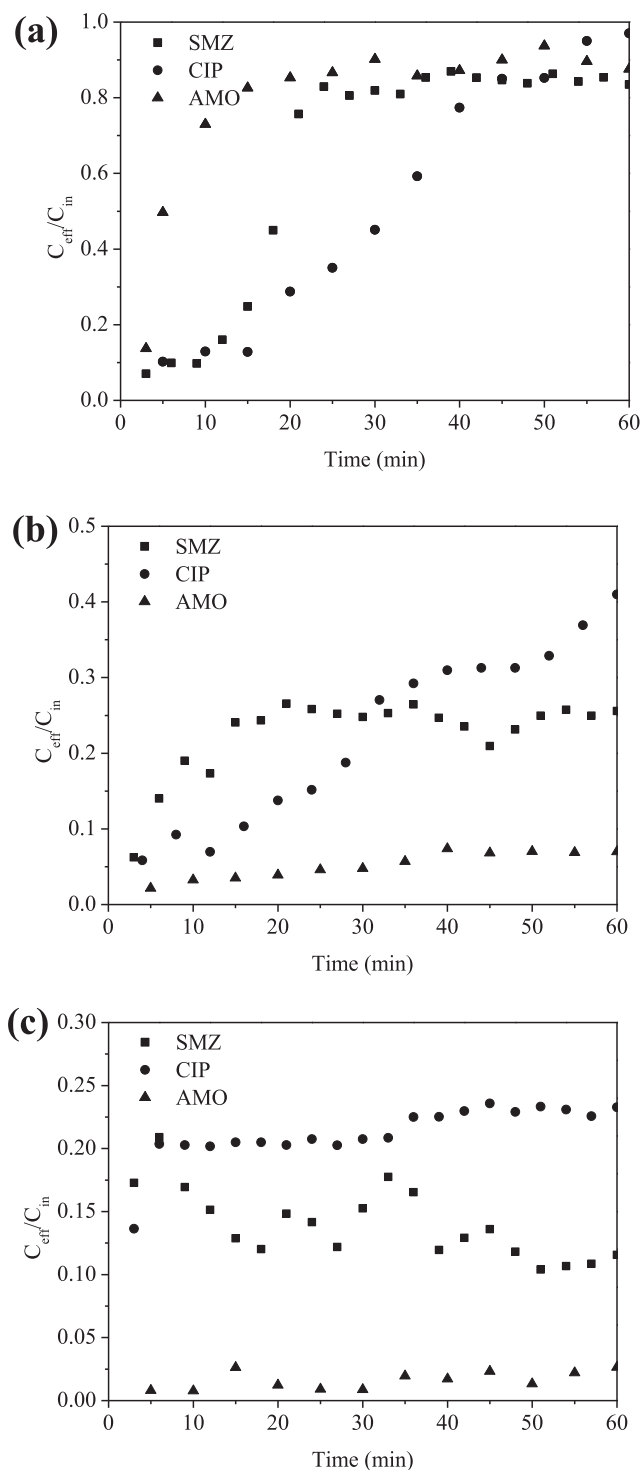**Fig. 3.** The different degradation ways for antibiotics (a) SMZ, (b) CIP, (c) AMO.

Fig. 4. Removing antibiotics using different ways (a) adsorption, (b) electrolysis, (c) MWCNT-based electrochemical membrane filtration.

followed by SMZ (90%) and CIP (76%). Compared to other electrochemical membrane filtration, it also showed excellent degradation efficiencies (displayed in Table S2).

3.3. Effects of cell voltage

The degradation efficiencies of SMZ, AMO and CIP at four different applied voltages (i.e., 0, 1, 2 and 3 V) using MWCNT-based electrochemical membrane filtration were investigated (displayed in Fig. 5).

Results showed that the steady-state effluent concentrations were achieved after 30 min, 50 min and 15 min for SMZ, CIP and AMO, respectively. Moreover, the removal efficiencies increased with the increasing voltage for all the antibiotics, which indicated that a stronger electric field resulted in more efficient degradation. Fig. 5a shows the results of electrochemical filtration of SMZ. It was noted that SMZ degradation efficiency at 1 V was nearly identical to that at 0 V, indicating that the voltage was too low to activate the production of reactive species on the surface of the MWCNT anode. The removal efficiencies were 70% and 90% at 2 and 3 V, respectively. The absence of SMZ
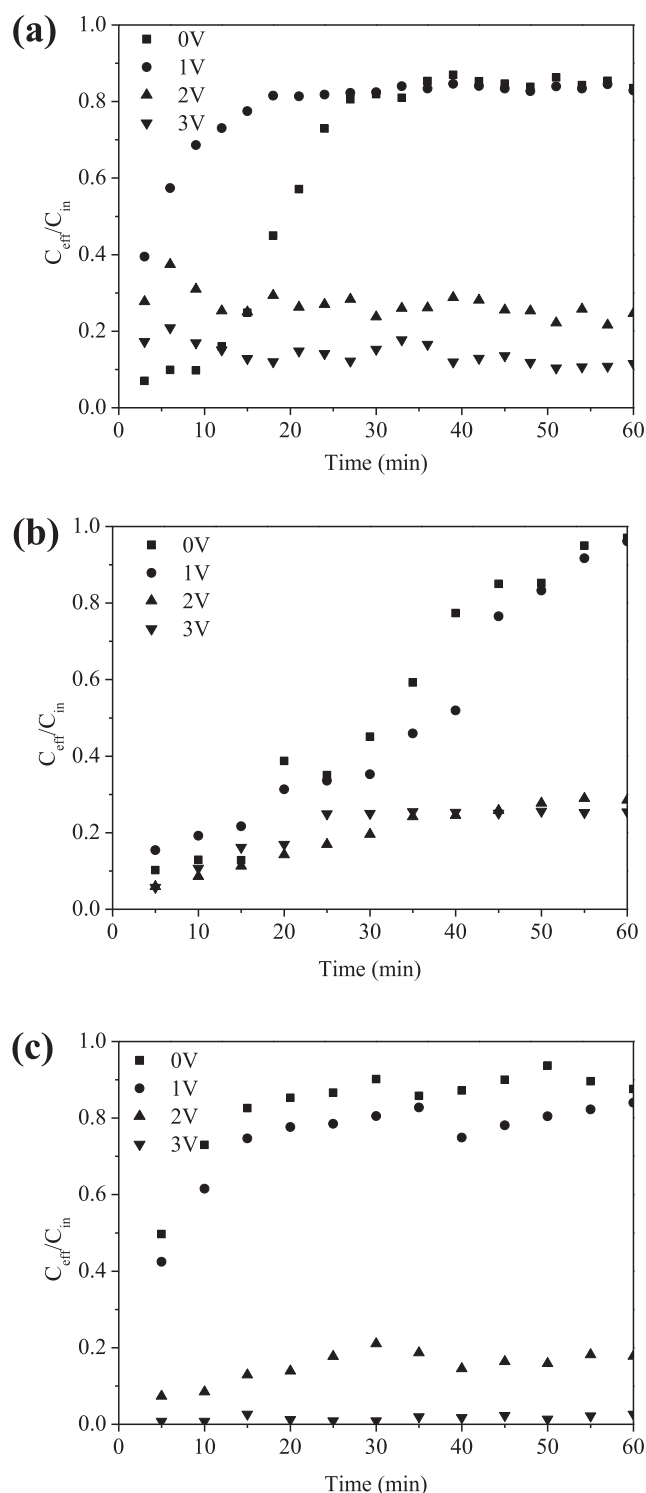
Fig. 5. Electrochemical membrane filtration of different antibiotics as a function of applied potential. (a) SMZ, (b) CIP, (c) AMO.

breakthrough at 2 and 3 V suggested that the main SMZ loss mechanism was oxidation. Fig. 5b shows the influence voltages on CIP removal efficiency. Results showed that the removal efficiency at 1 V was similar to that at 0 V, and the removal efficiency at 2 V was similar to that at 3 V. Fig. 5c shows that the application of 1 V results in a slight decay in AMO breakthrough as compared to 0 V conditions. The removal efficiencies for AMO were > 82% and > 98% at 2 and 3 V, respectively. The results were similar to SMZ and CIP electrochemical filtration results. Compared to the application of 0 V, the slight improvement

Table 1
Parameters of the pseudo-first-order kinetics (kapp) describing antibiotics removal.

Voltage (V)	SMZ		CIP		AMO	
	K_{app},s^{-1}	R^2	K_{app},s^{-1}	R^2	K_{app},s^{-1}	R^2
0	2.68E-03	0.716	5.04E-03	0.714	2.21E-03	0.964
1	2.92E-03	0.933	6.61E-03	0.630	2.90E-03	0.960
2	0.023	0.461	0.021	0.812	0.029	0.808
3	0.035	0.555	0.023	0.932	0.061	0.352

observed at 1 V was attributed to electrostatic attraction thus enhancing mass transfer by migration from bulk to surface [29]. However, compared to the application of 1 V, an obvious degradation was taking place at both 2 and 3 V. As the voltage increased, the number of generated electrons increased, the content of free radicals increased, and the removal rate of contaminants increased [38]. There is a conjugation effect and van der Waals force between antibiotics and MWCNTs, and the adsorption force is stronger. When the voltage is applied, the degradation rate of these antibiotics were greatly increased [45].

Overall, rapid removal of antibiotics in aqueous solution occurs when the charging voltage exceeded 2 V, and removal was inefficient when the voltage was decreased to 1 V. For MWCNT-based electrochemical membrane filtration, antibiotics remaining in the solution followed pseudo-first-order decay during the experiment (Eq. (1)).

$$\ln\left(\frac{c_t}{c_0}\right) = -k_{app}t \tag{1}$$

It was consistent with study of Zheng et al [47]. Apparent rate constants for antibiotics removal (k_{app}) as a function of voltage applied are shown in Table 1. A higher voltage led to a higher of the value of k_{app}. When the voltage was 3 V, the degradation velocity of these antibiotics was AMO (0.061 s^{-1}) > SMZ (0.035 s^{-1}) > CIP (0.023 s^{-1}). k_{app} at 0 V and 1 V were the same order of magnitude, k_{app} at 2 V and 3 V were the same order of magnitude. For example, k_{app} at 2 V and 3 V were 10 times of the 0 V and 1 V.

3.4. Different concentrations of antibiotics

The WWTPs concentration was far above at ppb level, even reaching ppm level. Therefore, three different concentrations (5 mg/L, 25 mg/L and 50 mg/L) of antibiotics were tested to investigate the degradation performance. Fig. 6 illustrates the removal efficiency of these antibiotics at different initial concentrations. It was observed that the removal efficiency of SMZ, CIP and AMO decreased from 90%, 75% and 99% to 51%, 43% and 16%, respectively, with the initial concentration of antibiotics increased from 5 mg/L to 50 mg/L. It is due to the fact that the same filtration volume and operating conditions of the electro-catalytic membrane, the amount of ·OH generation should be constant. Therefore, at higher initial concentrations, the limited and constant ·OH does not destroy much more antibiotic and its intermediates [46]. Hence, this appliance could adapt to pollution with low concentration and achieved high degradation efficiency. It could potentially be applied in practical antibiotic wastewater treatment.

3.5. Effects of pH and temperature

The pH and temperature are factors that might affect the electrochemical degradation of the membrane. Raising the temperature can decrease the solution viscosity and increase the mass transport rate from solution to the membrane surface, which will promote to generate more electrons and free radical, thus, much more ·OH will be produced to degrade antibiotics as well as it intermediates [39]. The pH is considered an important factor since it mostly affects the speciation of the pollutants and the redox potential of the generated oxidant.
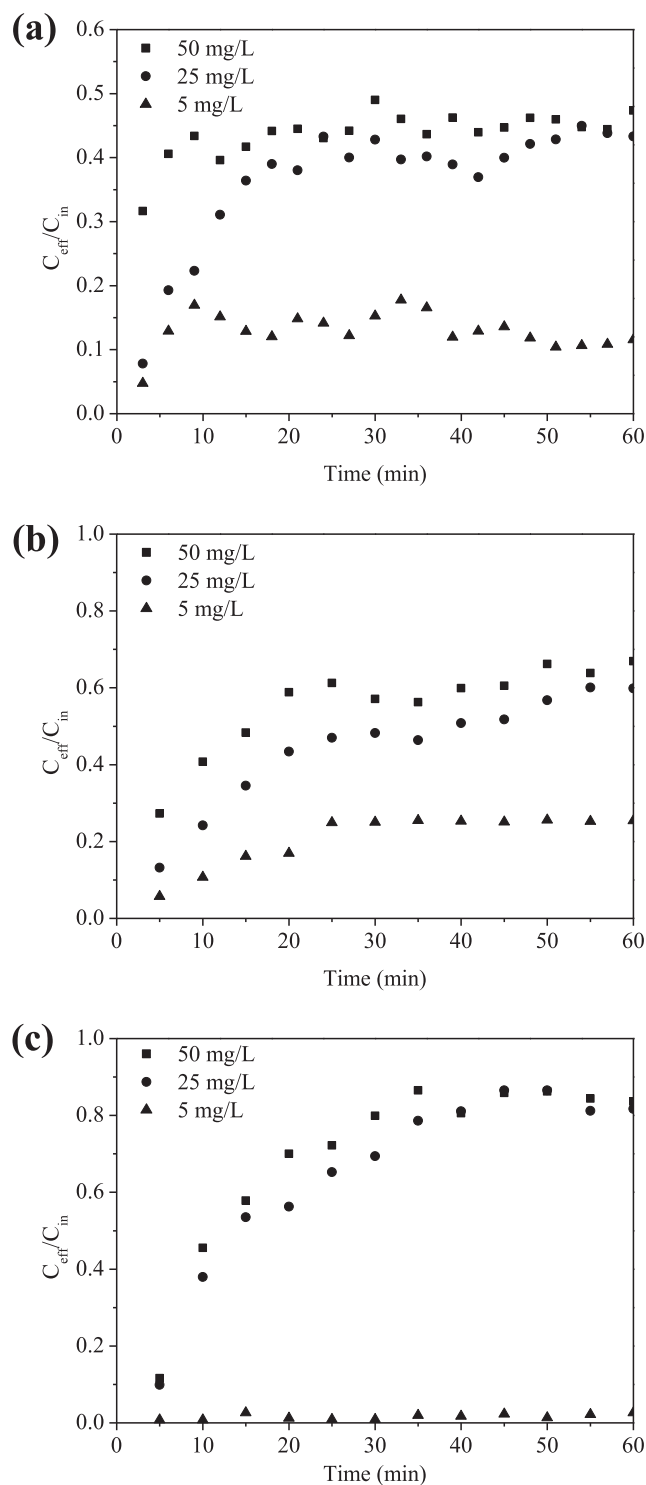
Fig. 6. (a) Degradation efficiencies of antibiotics with different initial concentrations using MWCNT-based electrochemical membrane filtration. (a) SMZ, (b) CIP, (c) AMO.

Fig. 7. Effect of pH on electrochemical membrane filtration degradation of antibiotics.

In order to elucidate whether these antibiotics can be effectively degraded in a wide pH range, electrochemical membrane filtration degradation of these antibiotics was conducted under five pH conditions (i.e., pH = 3, 5, 7, 9 and 11). As shown in Fig. 7, removal efficiencies for SMZ and AMO were almost independent on pH values. SMZ and AMO removal efficiencies were high and remain almost constant. However, electrochemical membrane filtration degradation of CIP was strongly pH-dependent. The r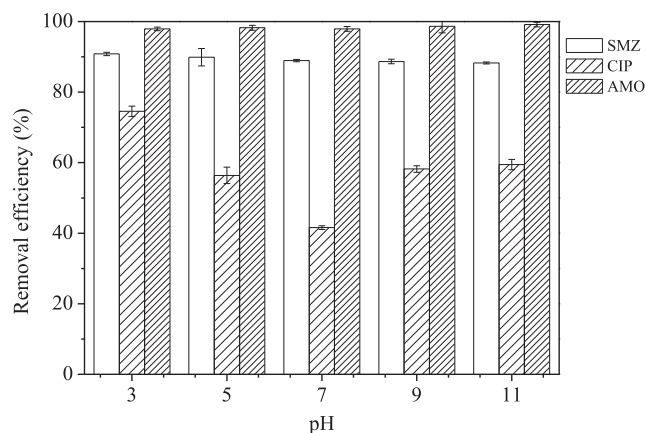emoval efficiency under acidic or alkaline environment was higher than that under neutral environment. The reason may be that target contaminant (i.e., SMZ, CIP and AMO) in the solution had different forms at different pH value (see Fig. 8), thus affecting the degradation mechanism of the pollutants [47,48]. For SMZ, when pH < pK_{a1}, the target contaminant was protonated and the molecule was positively charged, which prevented the unshared pair electrons delocalizing from N atom to aromatic ring and reduced their reactivity to electrophilic free radicals. When pH > pK_{a2}, −NH sulfonamide group deprotonated could reduce electron withdrawing effect on the aniline group, which enhanced its ability to radical oxidative activity [49]. It is well known that $\cdot$OH was an electron-deficient group belonging to an electrophile that attacked a negatively charged molecule [49]. Eqs. (2) and (3) shows that superoxide anions ($O_2^{\cdot-}$) would be favorably stable at a neutral to alkaline pH, the removal efficiency increased with a higher pH. While at an acidic pH, the formation of hydrogen peroxide (H_2O_2) would be favored [37]. Notably, when the pH of the solution decreased, the oxidation efficiency on the electrode surface decreased, and thereby enhanced the oxidation capacity of the system. In addition, low pH values also enhanced the effect of Cl^- on the removal efficiency of target pollutants, despite the low concentration of Cl^- in wastewater. When the pH value was 3, the main active chlorine substance was Cl_2. From pH 3 to 8, the dominant species was HClO. Because HClO (E° = 1.49 V/SHE) and Cl_2 (E° = 1.36 V/SHE) showed higher oxidation reduction potential than ClO^- (E° = 0.89 V/SHE), there was no doubt that the reaction in acidic solution can also be performed [50]. Therefore, whether it is acidic, neutral or basic, the removal efficiency can get to a decent state.

$$2O_2^{\cdot-} + H_2O \leftrightarrow HO_2^{\cdot} + OH^- \tag{2}$$

$$2O_2^{\cdot-} + 2H_2O \rightarrow 2OH^- + H_2O_2 + O_2 \tag{3}$$
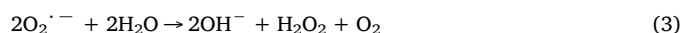
Temperature is associated with effluent treatment performance. In general, the removal efficiency increased with the increase of environment temperature, which was due to the increase in the adsorption and oxidation load [35]. As illustrated in the Fig. 9, increasing temperature could accelerate the degradation of contaminates. For example, SMZ removal efficiency was 77%, 90%, 96% at the temperature of 15 °C, 25 °C, 35 °C, respectively. Increasing the temperature could reduce the viscosity of the solution, thus increasing the mass transfer rate of the solution to the membrane surface, and generating more electrons and holes [39]. Therefore, more $\cdot$OH would be produced to degrade antibiotics and their intermediates. The effect of temperature on degradation efficiencies for these antibiotics was in the order SMZ > CIP > AMO.
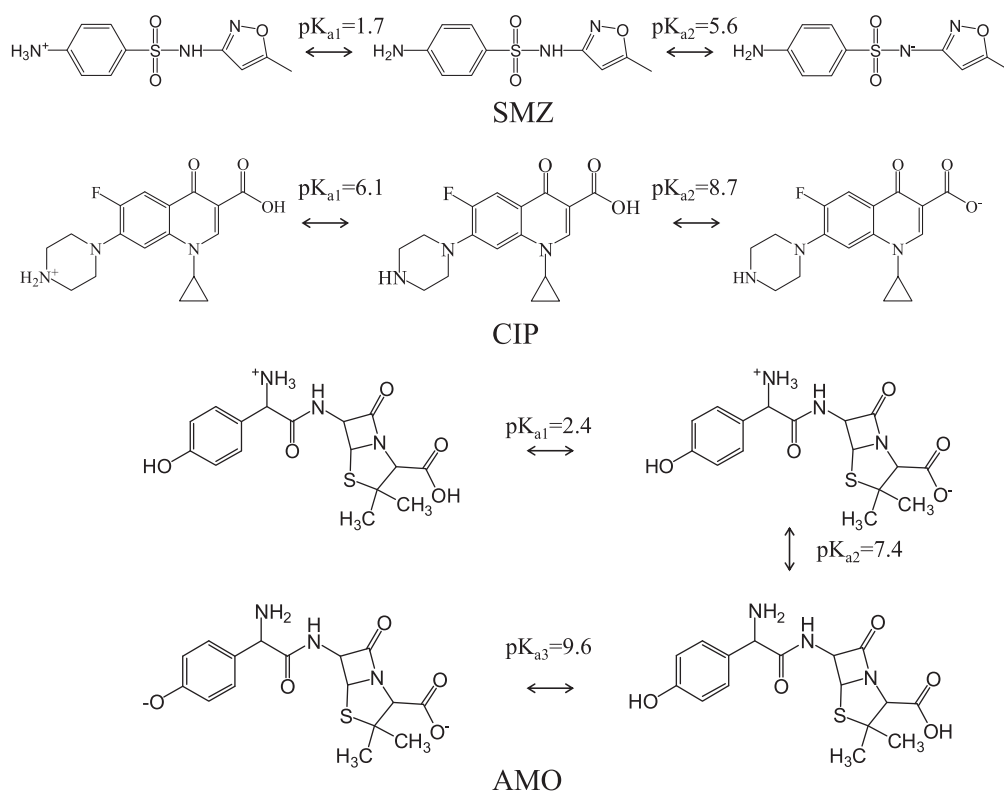
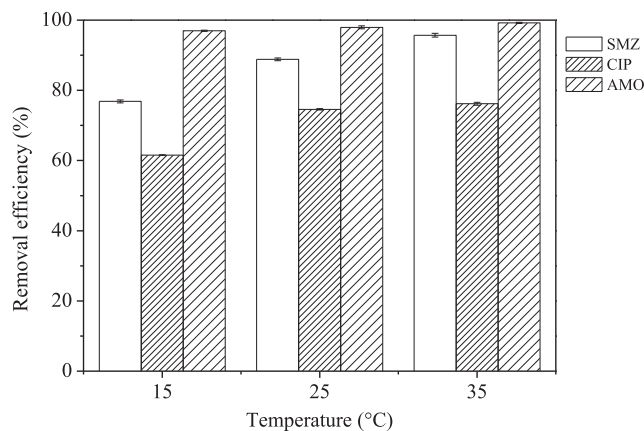**Fig. 8.** Different forms and pK$_a$ values of antibiotics.

Fig. 9. Effect of temperature on electrochemical membrane filtration degradation of antibiotics.

Fig. 10. Effect of SDBS on electrochemical membrane filtration degradation of antibiotics.

3.6. Effects of SDBS

SDBS, a typical representative of anionic surfactant, was widely used to increase the dispersity and stability of MWCNTs, and was selected as a model dissolved natural organic matter due to the prevalence of substances in surface water and wastewater effluent [51]. In our experiments, electrochemical membrane filtration process was conducted with the SDBS concentration of 5 mg/L. Results showed that antibiotics degradation in the presence of 5 mg/L SDBS was 7%, 8% and 1% lower than that without SDBS for SMZ, CIP and AMO, respectively (shown in Fig. 10). Among the targeted pollutants including AMO, SMZ and CIP, SDBS has the most significant effect on the degradation of CIP while it exhibited the weakest effect on AMO. This could be due to the specific molecular structure of SDBS. On the one hand, the strong π-π electron-donor-acceptor interaction between the benzene ring of SDBS molecule and the MWCNTs could compete for the absorption sites. On
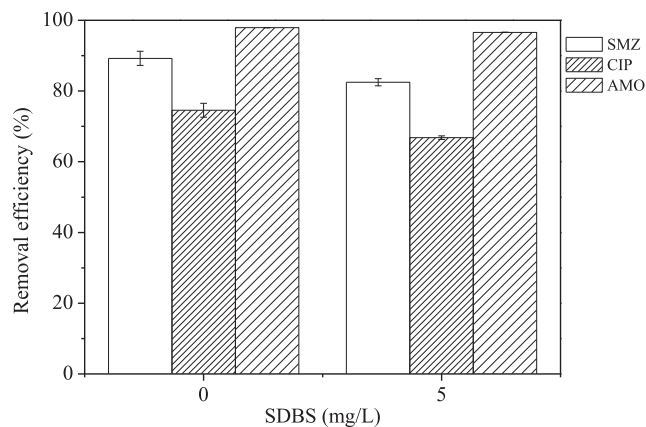
the other hand, the hydrophobic tail (12-carbon alkyl chain) of SDBS may be bound to the surface of MWCNTs through hydrophobic attraction. Song et al pointed out that the adsorption capacity of sediment for SDBS was enhanced as a result of the incorporation of MWCNTs [52]. So there may be a competitive relationship between SDBS and these antibiotics.

3.7. Reusability of membrane

Antibiotics may accumulate in the channels of the MWCNTs during degradation process, thus causing severe membrane fouling. MWCNT-based electrochemical filter membrane fouling was monitored by conducting four cycles of degradation experiments to examine the reusability of the filter membrane. All cycles were carried out with the same conditions (20 mM NaCl, 1.5 mL/min, 60 min). As shown in Fig. 11, the degradation efficiencies gradually decreased for all the three kinds of
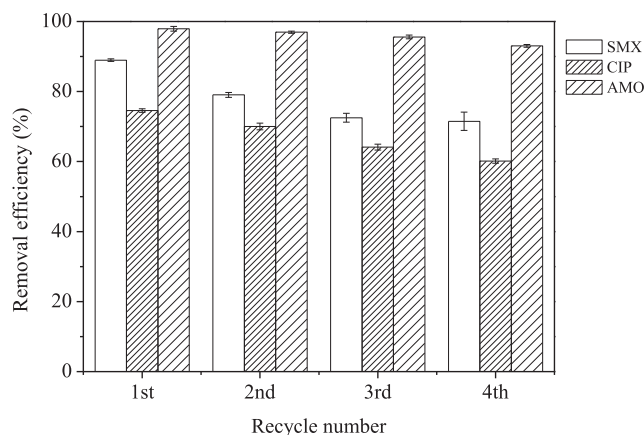
Fig. 11. Effect of recycle-index on electrochemical membrane filtration degradation of antibiotics.

antibiotics after each cycle of reuse. Noticeably, the removal efficiency was only 65%, 60% and 90% at the 4th cycle for SMZ, CIP and AMO, respectively, which exhibited 72%, 79% and 92% degradation performance for SMZ, CIP and AMO, respectively, when compared to the first cycle. Among them, AMO had the highest degradation efficiency. The loss of degradation efficiency was probably attributed to the high molar mass products formed during SMZ and CIP oxidation as described later, which could accumulate and jam the membrane access and bring about higher mass transfer resistance [23]. The degradation ability of these antibiotics was: AMO > SMZ > CIP. This result indicated that the MWCNT membrane had excellent reusability for electrochemical degradation, and this membrane has potential for practical applications.

3.8. Effects of simultaneous removal of SMZ, CIP, and AMO

Under the optimal parameter conditions in electric filtration, the removal of mixed contamination experiments was conducted to determine the combined removal effects. As illustrated in Fig. 12, this group of experiments was divided into four categories. In Fig. 12a, binary mixtures of SMZ and AMO were decomposed simultaneously, AMO was nearly completely removed, and SMZ was only removed 60% within 60 min. SMZ and CIP were also degraded simultaneously (shown in Fig.e 12b,). Results showed that both SMZ and CIP were nearly completely removed within 60 min. Nevertheless, the effluent concentrations of CIP and AMO binary solution were both remained 12% after 60 min (displayed in Fig. 12c). Ternary systems were also investigated in which SMZ, CIP and AMO were simultaneously added to the apparats (shown in Fig. 12d). Results showed that SMZ and AMO could be removed thoroughly, while CIP was only removed 20%. In the experiments, SMZ, CIP and AMO can be simultaneously removed at different degree. It was supposed that degradation of AMO was the most simple owing to its structure, the next was SMZ, the most difficult to be removed was CIP. Different molecular configuration led to different electrochemical filtration behaviors. From the perspective of chemical structure, AMO lactam ring was easily affected by external chemical environment, such as acid, alkali, heat, nucleophile attack, which was prone to degradation by opening loop [53]. In addition, multiple chiral centers and unsaturated double bonds made AMO were prone to isomerization [54]. Moreover, some chemical structures of the side chains were also prone to degradation or isomerization [7]. Considering the different molecular structures, the discrepancy in the degradation between SMZ and CIP can be explained. Since SMZ was comprised of benzene and isoxazole ring with chain linkage whereas CIP had piperazine and quinolone ring connected by short connection, the electron density of SMZ was expected to be lower than CIP [55]. In this system, ·OH played a more important role in SMZ and CIP oxidation. A theoretical calculation indicated that the N−S bond, C−N bond, C−S bond, and the C−C bond (benzene ring) in SMZ molecule, were easily broken by the attack of ·OH [56], while another calculation shows that the reaction site of ·OH attack CIP was C−F bond, C−N bond and C−C bond (benzene ring) [57]. Thus, compared to SMZ, CIP degradation by MWCNTs-based electrochemical membrane filtration was found to be less efficient.
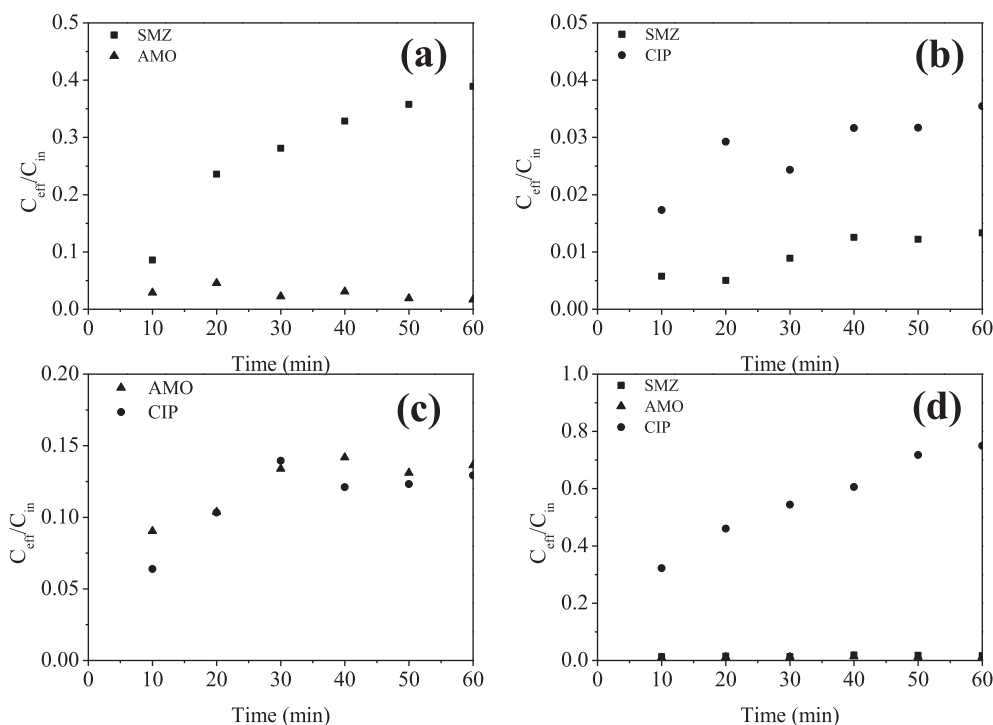

Fig. 12. Simultaneously remove different antibiotics using MWCNT-based electrochemical membrane filtration. (a) SMZ and AMO binary mixture; (b) SMZ and CIP binary mixture; (c) AMO and CIP binary mixture; (d) SMZ, CIP and AMO ternary mixture.

Table 2

Identification of the main intermediates compounds formed in the electrochemical degradation of antibiotics and their respective chemical structures elucidated by the LC–MS technique. (a) SMZ, (b) CIP and (c) AMO.

(a)

Compound	M-H	Identification	Chemical structure
1	283	$C_{10}H_9N_3O_5S$	
2	273	$C_8H_7N_3O_6S$	
3	245	$C_7H_7N_3O_5S$	
4	122	$C_6H_4NO_2$	
5	271	$C_{10}H_{11}N_2O_5S$	
6	288	$C_{10}H_{12}N_2O_6S$	
7	216	$C_7H_8N_2O_4S$	
8	139	$C_6H_5NO_3$	
9	132	$C_4H_8N_2O_3$	
10	117	$C_4H_7NO_3$	
11	178	$C_4H_6N_2O_4S$	
SMZ	253	$C_{10}H_{11}N_3O_3S$	
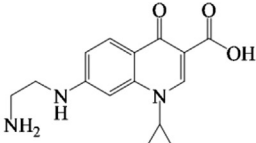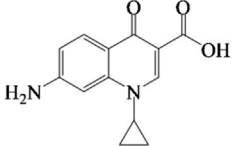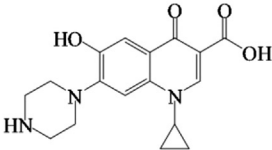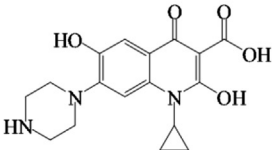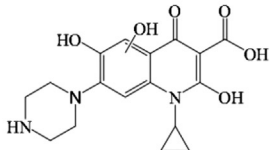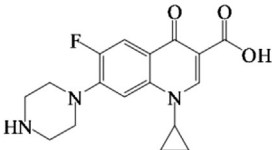
Table 2 (*continued*)

(b)

Compound	M–H	Identification	Chemical structure
1	309	$C_{14}H_{13}FN_2O_5$	
2	364	$C_{17}H_{18}FN_3O_5$	
3	396	$C_{17}H_{19}FN_3O_7$	
4	362	$C_{17}H_{16}FN_3O_5$	
5	346	$C_{17}H_{16}FN_3O_4$	
6	343	$C_{17}H_{16}N_3O_5$	
7	327	$C_{17}H_{16}N_3O_4$	

Table 2 (*continued*)

8	312	$C_{17}H_{17}N_3O_3$	
9	245	$C_{13}H_{12}N_2O_3$	
10	330	$C_{17}H_{19}N_3O_4$	
11	346	$C_{17}H_{19}N_3O_5$	
12	362	$C_{17}H_{20}N_3O_6$	
CIP	332	$C_{17}H_{18}FN_3O_3$	

Table 2 (*continued*)

(c)	Compound	M-H	Identification	Chemical structure
	1	381	$C_{16}H_{19}N_3O_6S$	
	2	397	$C_{16}H_{19}N_3O_7S$	
	3	383	$C_{16}H_{21}N_3O_6S$	
	4	339	$C_{15}H_{21}N_3O_4S$	
	5	138	$C_7H_6O_3$	
	6	244	$C_9H_{12}N_2O_4S$	
	7	195	$C_5H_9NO_5S$	
	AMO	365	$C_{16}H_{19}N_3O_5S$	

3.9. Identification of transformation by-products

There are 11 intermediates had been detected through LC-MS analysis during SMZ degradation by electrochemical membrane filtration. All intermediates compounds identified were given in Table 2a and proposed a possible oxidation mechanism. The main reaction pathways were summarized in Fig. 13a.

The first pathway was the oxidation of amino groups of benzene ring and the formation of the nitro-derivative of SMZ. Compound C1 yielded an *m/z* ratio of 284. There was a large body of literature that indicated that the amino group was oxidized to nitro [58-60]. Then the

opening of the isoxazole ring was assessed by identifying compound C2. Afterwards, the loss of one carbonyl group generated the intermediate C3 at the *m/z* of 246. It was obvious that the mass spectrum C3 increased significantly at 40 min and decreased at 60 min, indicating that it was a characteristic intermediate product. Due to the strong electron-withdrawing effect of the nitro group, the nitro group was conjugated to the benzene ring, then the link between the benzene ring and the sulfur disconnected, so compound C4 was gained. The second pathway involved the attack of the hydroxyl radical on the isoxazole ring and then the substitution of the amino group by a hydroxyl group in the benzene ring, which was at the *m/z* of 271 (C5), which was in line with
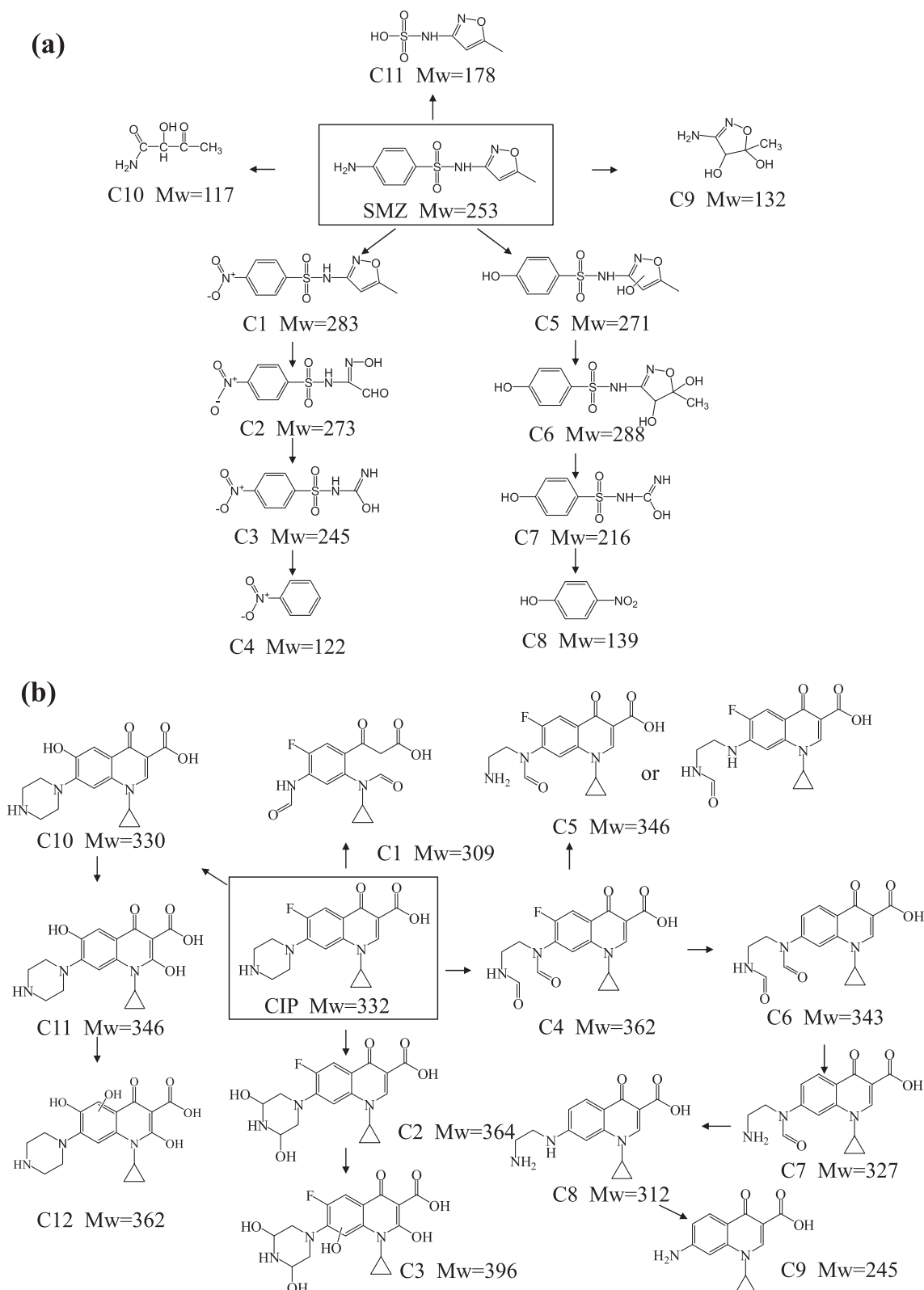
(a)

(b)

Fig. 13. Degradation pathways for different antibiotics during MWCNTs electrochemical membrane filtration. (a) SMZ, (b) CIP, (c) AMO.

the previous reports [61]. Then owing to the attack of ·OH radicals to the double bond on the isoxazole ring, the dihydroxylated compound C6 was formed. This intermediate was the same as C3, with a maximum yield of 40 min and a decrease of 60 min, suggesting that the pathway was reliable. The opening of the isoxazole ring and taking out one molecule of carbonyl was figured out by recognizing compound C7.

Ultimately, compound C8 was formed at the *m/z* of 140. The third pathway was that, the sulfonamide S−N bond of SMZ was readily cleaved by the attack of oxidizing species, leading to the formation of C9. As to the formation of C10 at the *m/z* of 118 was due to the attack of ·OH radicals, and the formation of C11 at the *m/z* of 179, similar intermediates had also been identified in photocatalytic degradation
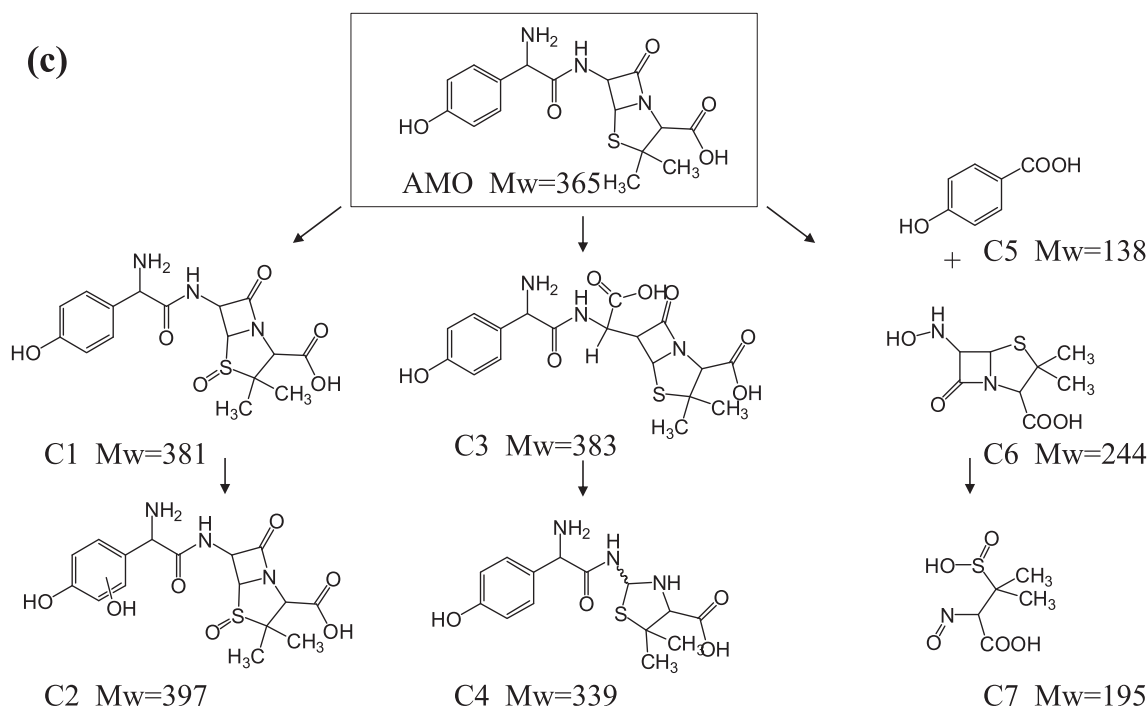
14

Fig. 13. (*continued*)

reported by Ioannidou et al [58].

Judging from the identified by-products, the following reaction pathways for CIP degradation were proposed (shown in Fig. 13b). There were 12 intermediates that had been detected through LC–MS analysis during CIP degradation by our methods. All intermediates compounds identified were given in Table 2b and a possible oxidation mechanism was proposed.

Degradation was mainly due to two reasons. On one hand, oxidation of quinolones occurred thus leading to defluorination and hydroxyl substitution reactions. On the other hand, the reaction at the piperazinyl ring was taken place [62]. The similar degradation mechanism was also proposed by some studies using either electrochemical oxidation or activated-persulfate degradation [55,63,64]. In our work, both mechanisms described above were put forward simultaneously. Reaction at the stepwise oxidative degradation of the piperazinyl side chain was found 10 kinds of compounds. The oxidation of the piperazinyl leaded to ring opening, generating the di-aldehyde derivative *m/z* 362 C4. Then, the degradation was continued in two ways. The loss of one formaldehyde group of the piperazinyl group after oxidation to obtain two isomers C5, and the other was defluorination on the quinolone group to obtain C6. Then the piperazinyl group gradually removed the formaldehyde group to obtain C7 and C8, respectively, followed by the loss of formaldehyde from amine side chain to obtain C9. The secondary pathway was the self-sensitized oxidation of quinolone ring, followed by decarbonization and N-dealkylation on piperazine ring, and product C1 was obtained. The third pathway appeared to take place via the addition of two oxygen atom that produced the dihydroxy derivative of piperazinyl ring (C2), and then with another hydroxyl radical addition to the parent molecule get C3. The fourth pathway was the intermediate product, C10, resulted from hydroxyl radical attacking at the fluorine atom, followed by the hydroxylation resulting in the formation of C11 and C12, successively.

Analysis by LC–MS allowed the detection and identification of 7 intermediates during AMO degradation. All intermediates compounds identified were given in Table 2c and a possible oxidation mechanism was proposed. The main reactions pathways were summarized in Fig. 13c.

Degradation was mainly owing to three kinds of reasons. The first

was due to the fracture of the β-lactam ring, the second was due to the oxidation of sulfur atom, and the third was cracked at the aromatic [65–67]. In our research, the first pathway began with the attack of oxidants (e.g., HO˙, Cl˙) on sulfur atom of AMO, resulting in the formation and hydroxylation of the sulfoxide derivatives (C1) and successively forming complex compound (C2). Another pathway was initialized by the destruction of the four-membered β-lactam ring, thus yielding the penicilloic acid (C3), which contained a free carboxylic acid group. Decarboxylation of the free carboxylic acid occurred and generated the intermediate C4. The third degradation pathway was formed by the cleavage of AMO molecules on peptide bonds closer to the aromatic ring to form p- hydroxybenzoic acid (C5) and a dicyclolactam product C6. Then C6 was degraded into an open-chain structure (C7).

3.10. The electrochemical filtration mechanism

The organic electrochemical filtration reaction mechanism followed a multi-step process: firstly, deposition and adsorption of antibiotics onto the electrode surface (Ep. (4)). Secondly, antibiotics degraded and molecular transformed. The electrochemical filter degradation of antibiotics may occur through two primary mechanisms, the direct oxidation of antibiotics in contact with MWCNTs anode, and the indirect oxidation of antibiotics through anodic production of some aqueous oxidants (e.g., HO˙, Cl˙) [18,31,32,35,36,68]. These antibiotics degradation mechanisms were shown in Fig. 14. Direct oxidation was the oxidation of antibiotics adhered to the MWCNTs electrochemical filter, which was an electron process (Ep. (5)). Indirect oxidation possessed two steps. The first step produced some solvated radicals on the anode (Ep. (6)). The second step was that antibiotics were oxidized by the produced oxidants step by step (Ep. (7)). According to the previous research, when anodic potential < 0.8 V, direct oxidation played the main role in the system, once the anodic potential was increased to > 0.95 V, the effluent concentration began to decrease with increasing potential indicating that indirect and direct oxidation occurred simultaneously [38]. Thirdly, the degradation product exfoliated. In addition, the degradation of antibiotics partly might be caused by electrocoagulation due to the dissolution of the porous stainless steel.
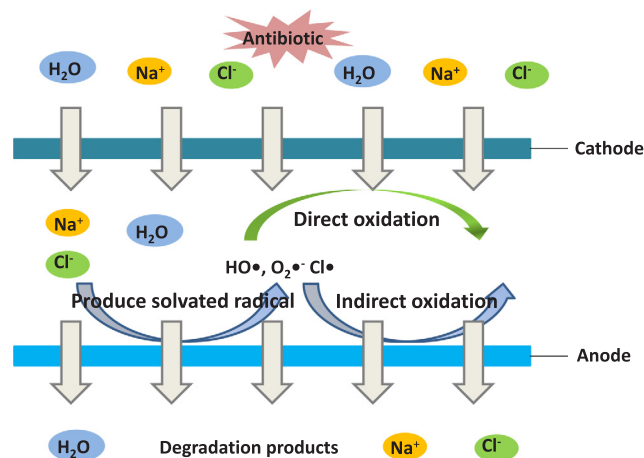
$$\text{Antibiotics + MWCNTs} \rightarrow \text{Antibiotics} \cdots \text{MWCNTs} \tag{4}$$
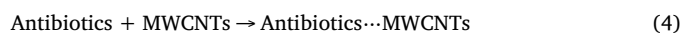
Fig. 14. The proposed mechanism of antibiotics oxidation during electrochemical filter oxidation.
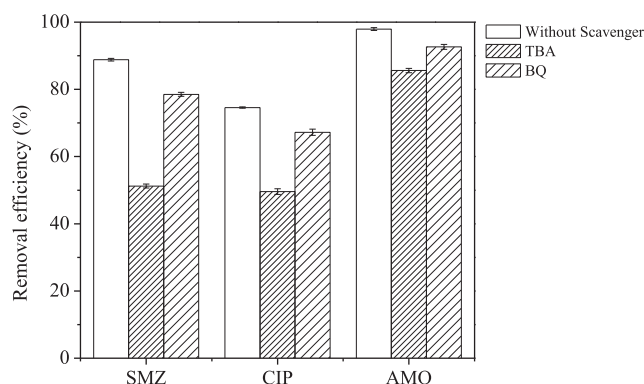
Fig. 15. Influence of TBA and BQ on the electrochemical oxidation of different antibiotics.

$$Antibiotics\cdots MWCNTs + e^- \rightarrow Degradation\ products \qquad (5)$$

$$MWCNTs + Ox^- (H_2O, Cl^-) \rightarrow MWCNTs + Ox^{\cdot} (HO^{\cdot}, O_2^{\cdot\,-} Cl^{\cdot}) \qquad (6)$$

$$Antibiotics + Ox^{\cdot} (HO^{\cdot}, O_2^{\cdot\,-} Cl^{\cdot}) \rightarrow Degradation\ products \qquad (7)$$
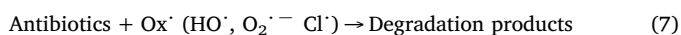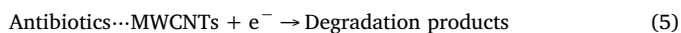
In order to determine the effect of the indirect pathway on the electrochemical oxidation of antibiotics on MWCNTs electrode, the relevant experiments were conducted by adding appropriate radical scavengers. Tertiary butanol (TBA) with concentration of 5 mM was used as the $HO^{\cdot}$ radicals scavenger and 5 mM benzoquinone (BQ) was used as $O_2^{\cdot\,-}$ radicals scavenger. As shown in Fig. 15, SMZ removal efficiency decreased 37.6% by adding TBA while it decreased 10.3% by adding BQ, CIP removal efficiency decreased 25.1% by adding TBA while it decreased 7.5% by adding BQ, AMO removal efficiency decreased 12.3% by adding TBA while it decreased 5.2% by adding BQ, which meaned that the $HO^{\cdot}$ radicals accounted for the primary role of indirect electrochemical oxidation for antibiotics degradation and the effect of $O_2^{\cdot\,-}$ radial just played subsidiary role.

4. Conclusions

In this work, three kinds of antibiotics including SMZ, CIP and AMO were simultaneously removed in binary and ternary systems using electrochemical filter. The main conclusions were as follows: (1) MWCNT-based electrochemical membrane filtration comprised of a composite conductive electrochemical filter membrane anode and a stainless steel network cathode. (2) After 60 min of electrochemical filtration process, in single system, degradation of SMZ, CIP and AMO

was 90%, 76% and 98%, respectively. In both binary and ternary systems, degradation efficiencies were in the order of AMO > SMZ > CIP. (3) Degradation efficiency was enhanced by increasing the voltage and temperature, while it decreased with the increased initial concentration and the addition of SDBS. The degradation efficiencies of SMZ and AMO were independent on solution pH. However, the degradation efficiency of CIP was higher in acidic or alkaline than that in neutral solution. It still exhibited good antibiotics degradation efficiency after four time cycles reuse. (4) Hydroxylation, cleavage of sulfonamide S−N bond and oxidation of aniline moiety were found to be the major pathways, which was responsible for SMZ degradation. The oxidation of quinolone ring and the reaction at the piperazinyl ring were the major pathways of CIP. The fracture of the β-lactam ring, the oxidation of sulfur atom and the crack at the aromatic were the reasons of AMO degradation. (5) Both direct oxidation and indirect oxidation affected the degradation of antibiotics. In summary, MWCNT-based electrochemical membrane filtration was successful in degrading multiple antibiotics and this study offers a promising technology to lessen the hazardous effects of multiple antibiotics in nature.

Declaration of Competing Interest

The authors declared that there is no Conflict of Interest.

Appendix A. Supplementary material

Supplementary data to this article can be found online at https://doi.org/10.1016/j.seppur.2019.116167.

References

[1] C. Zhang, D. Tian, X. Yi, T. Zhang, J. Ruan, R. Wu, C. Chen, M. Huang, G. Ying, Occurrence, distribution and seasonal variation of five neonicotinoid insecticides in surface water and sediment of the Pearl Rivers, South China, Chemosphere 217 (2019) 437–446.

[2] K. He, Z. Zeng, A. Chen, G. Zeng, R. Xiao, P. Xu, Z. Huang, J. Shi, L. Hu, G. Chen, Advancement of Ag–graphene based nanocomposites: an overview of synthesis and its applications, Small 14 (2018) 1800871.

[3] X. Yi, C. Zhang, H. Liu, R. Wu, D. Tian, J. Ruan, T. Zhang, M. Huang, G. Ying, Occurrence and distribution of neonicotinoid insecticides in surface water and sediment of the Guangzhou section of the Pearl River, South China, Environ Pollut 251 (2019) 892–900.

[4] S. Ye, M. Yan, X. Tan, J. Liang, G. Zeng, H. Wu, B. Song, C. Zhou, Y. Yang, H. Wang, Facile assembled biochar-based nanocomposite with improved graphitization for efficient photocatalytic activity driven by visible light, Appl. Catal. B: Environ. (2019).

[5] W. Wang, P. Xu, M. Chen, G. Zeng, C. Zhang, C. Zhou, Y. Yang, D. Huang, C. Lai, M. Cheng, L. Hu, W. Xiong, H. Guo, M. Zhou, Alkali metal-assisted synthesis of graphite carbon nitride with tunable band-gap for enhanced visible-light-driven photocatalytic performance, ACS Sust. Chem. Eng. 6 (2018) 15503–15516.

[6] B. Qingwei, W. Bin, D. Jun, D. Shubo, Y. Gang, Pharmaceuticals and personal care products in the aquatic environment in China: a review, J. Hazard. Mater. 262C (2013) 189.

[7] I.T. Carvalho, L. Santos, Antibiotics in the aquatic environments: a review of the European scenario, Environ. Int. 94 (2016) 736–757.

[8] Z. Qian-Qian, Y. Guang-Guo, P. Chang-Gui, L. You-Sheng, Z. Jian-Liang, Comprehensive evaluation of antibiotics emission and fate in the river basins of china: source analysis, multimedia modeling, and linkage to bacterial resistance, Environ. Sci. Technol. 49 (2015) 6772–6782.

[9] R. Gothwal, T. Shashidhar, Antibiotic pollution in the environment: a review, CLEAN-Soil, Air, Water 43 (2015) 479–489.

[10] S. Suzuki, P.T. Hoa, Distribution of quinolones, sulfonamides, tetracyclines in aquatic environment and antibiotic resistance in indochina, Front. Microbiol. 3 (2012) 67.

[11] S. Ye, G. Zeng, H. Wu, C. Zhang, J. Liang, J. Dai, Z. Liu, W. Xiong, J. Wan, P. Xu, Co-occurrence and interactions of pollutants, and their impacts on soil remediation—a

review, Crit. Rev. Environ. Sci. Technol. 47 (2017) 1528–1553.

[12] Z.H. Wen, L. Chen, X.Z. Meng, Y.P. Duan, Z.S. Zhang, E.Y. Zeng, Occurrence and human health risk of wastewater–derived pharmaceuticals in a drinking water source for Shangha, East China, Sci. Total Environ. 490 (2014) 987–993.

[13] V. Homem, L. Santos, Degradation and removal methods of antibiotics from aqueous matrices – a review, J. Environ. Manage. 92 (2011) 2304–2347.

[14] K.J. Choi, S.G. Kim, S.H. Kim, Removal of antibiotics by coagulation and granular activated carbon filtration, J. Hazard. Mater. 151 (2008) 38–43.

[15] Y. Yang, C. Zhang, C. Lai, G. Zeng, D. Huang, M. Cheng, J. Wang, F. Chen, C. Zhou, W. Xiong, BiOX (X= Cl, Br, I) photocatalytic nanomaterials: applications for fuels and environmental management, Adv. Colloid Interface Sci. 254 (2018) 76–93.

[16] L. Zhang, J. Zhang, G. Zeng, H. Dong, Y. Chen, C. Huang, Y. Zhu, R. Xu, Y. Cheng, K. Hou, Multivariate relationships between microbial communities and environmental variables during co-composting of sewage sludge and agricultural waste in the presence of PVP-AgNPs, Bioresour. Technol. 261 (2018) 10–18.

[17] H. Wang, Z. Zeng, P. Xu, L. Li, G. Zeng, R. Xiao, Z. Tang, D. Huang, L. Tang, C. Lai, Recent progress in covalent organic framework thin films: fabrications, applications and perspectives, Chem. Soc. Rev. 48 (2019) 488–516.

[18] P. Liu, H. Zhang, Y. Feng, C. Shen, F. Yang, Integrating electrochemical oxidation into forward osmosis process for removal of trace antibiotics in wastewater, J. Hazard. Mater. 296 (2015) 248–255.

[19] F. Sopaj, M.A. Rodrigo, N. Oturan, F.I. Podvorica, J. Pinson, M.A. Oturan, Influence of the anode materials on the electrochemical oxidation efficiency. Application to oxidative degradation of the pharmaceutical amoxicillin, Chem. Eng. J. 262 (2015) 286–294.

[20] S.O. Ganiyu, N. Oturan, S. Raffy, M. Cretin, R. Esmilaire, E. van Hullebusch, G. Esposito, M.A. Oturan, Sub-stoichiometric titanium oxide (Ti₄O₇) as a suitable ceramic anode for electrooxidation of organic pollutants: A case study of kinetics, mineralization and toxicity assessment of amoxicillin, Water Res. 106 (2016) 171–182.

[21] M. Panizza, A. Dirany, I. Sirés, M. Haidar, N. Oturan, M.A. Oturan, Complete mineralization of the antibiotic amoxicillin by electro-Fenton with a BDD anode, J. Appl. Electrochem. 44 (2014) 1327–1335.

[22] B.G. Padilla-Robles, A. Alonso, S.A. Martinez-Delgadillo, M. Gonzalez-Brambila, U.J. Jauregui-Haza, J. Ramirez-Munoz, Electrochemical degradation of amoxicillin in aqueous media, Chem. Eng. Process. 94 (2015) 93–98.

[23] C. Ji, J. Hou, V. Chen, Cross-linked carbon nanotubes-based biocatalytic membranes for micro-pollutants degradation: performance, stability, and regeneration, J. Membr. Sci. 520 (2016) 869–880.

[24] Y.F. Wang, H.O. Huang, X.M. Wei, Influence of wastewater precoagulation on adsorptive filtration of pharmaceutical and personal care products by carbon nanotube membranes, Chem. Eng. J. 333 (2018) 66–75.

[25] M. Liu, Y. Liu, D. Bao, G. Zhu, G. Yang, J. Geng, H. Li, Effective Removal of Tetracycline Antibiotics from Water using Hybrid Carbon Membranes, Sci. Rep. 7 (2017) 43717.

[26] Y.F. Wang, J.X. Zhu, H.O. Huang, H.H. Cho, Carbon nanotube composite membranes for microfiltration of pharmaceuticals and personal care products: capabilities and potential mechanisms, J. Membr. Sci. 479 (2015) 165–174.

[27] H. Wu, X.J. Niu, J. Yang, C.H. Wang, M.Q. Lu, Retentions of bisphenol A and norfloxacin by three different ultrafiltration membranes in regard to drinking water treatment, Chem. Eng. J. 294 (2016) 410–416.

[28] J. Lee, S. Jeong, Y. Ye, V. Chen, S. Vigneswaran, T. Leiknes, Z.W. Liu, Protein fouling in carbon nanotubes enhanced ultrafiltration membrane: fouling mechanism as a function of pH and ionic strength, Sep. Purif. Technol. 176 (2017) 323–334.

[29] A.R. Bakr, M.S. Rahaman, Electrochemical efficacy of a carboxylated multiwalled carbon nanotube filter for the removal of ibuprofen from aqueous solutions under acidic conditions, Chemosphere 153 (2016) 508–520.

[30] J.-L. Gong, B. Wang, G.-M. Zeng, C.-P. Yang, C.-G. Niu, Q.-Y. Niu, W.-J. Zhou, Y. Liang, Removal of cationic dyes from aqueous solution using magnetic multi-wall carbon nanotube nanocomposite as adsorbent, J. Hazard. Mater. 164 (2009) 1517–1522.

[31] Z. Pan, C. Song, L. Li, H. Wang, Y. Pan, C. Wang, J. Li, T. Wang, X. Feng, Membrane technology coupled with electrochemical advanced oxidation processes for organic wastewater treatment: recent advances and future prospects, Chem. Eng. J. (2019).

[32] S.O. Ganiyu, E.D. van Hullebusch, M. Cretin, G. Esposito, M.A. Oturan, Coupling of membrane filtration and advanced oxidation processes for removal of pharmaceutical residues: a critical review, Sep. Purif. Technol. 156 (2015) 891–914.

[33] Z.Z. Chowdhury, S. Sagadevan, R. Bin Johan, S.T. Shah, A. Adebesi, S. IslamMd, R.F. Rafique, A review on electrochemically modified carbon nanotubes (CNTs) membrane for desalination and purification of water, Mater. Res. Express 5 (2018) 102001.

[34] G. Gao, C.D. Vecitis, Doped carbon nanotube networks for electrochemical filtration of aqueous phenol: electrolyte precipitation and phenol polymerization, ACS Appl. Mater. Interfaces 4 (2012) 1478–1489.

[35] H. Liu, C.D. Vecitis, Reactive transport mechanism for organic oxidation during electrochemical filtration: mass-transfer, physical adsorption, and electron-transfer, J. Phys. Chem. C 116 (2016) 374–383.

[36] C.D. Vecitis, M.H. Schnoor, M.S. Rahaman, J.D. Schiffman, M. Elimelech, Electrochemical multiwalled carbon nanotube filter for viral and bacterial removal and inactivation, Environ. Sci. Technol. 45 (2011) 3672–3679.

[37] A.R. Bakr, M.S. Rahaman, Removal of bisphenol A by electrochemical carbon-nanotube filter: Influential factors and degradation pathway, Chemosphere 185 (2017) 879–887.

[38] L. Yanbiao, L. Han, Z. Zhi, W. Tianren, O. Choon Nam, C.D. Vecitis, Degradation of the common aqueous antibiotic tetracycline using a carbon nanotube electrochemical filter, Environ. Sci. Technol. 49 (2015) 7974–7980.

[39] L. Zhimeng, Z. Mengfu, W. Zheng, W. Hong, D. Cheng, L. Kui, Effective Degradation

of Aqueous Tetracycline Using a Nano-TiO2/Carbon Electrocatalytic Membrane, Materials.

[40] F. Li, Q. Xia, Q.X. Cheng, M.Z. Huang, Y.B. Liu, Conductive cotton filters for affordable and efficient water purification, Catalysts 7 (2017) 291.

[41] C. Trellu, C. Coetsier, J.C. Rouch, R. Esmilaire, M. Rivallin, M. Cretin, C. Causserand, Mineralization of organic pollutants by anodic oxidation using reactive electrochemical membrane synthesized from carbothermal reduction of TiO2, Water Res 131 (2018) 310–319.

[42] A.M. Zaky, B.P. Chaplin, Mechanism of p-substituted phenol oxidation at a Ti₄O₇ reactive electrochemical membrane, Environ. Sci. Technol. 48 (2014) 5857–5867.

[43] C.D. Vecitis, G. Gao, H. Liu, Electrochemical carbon nanotube filter for adsorption, desorption, and oxidation of aqueous dyes and anions, J. Phys. Chem. C 115 (2011) 3621–3629.

[44] Z. Niu, Y. Wang, H. Lin, F. Jin, Y. Li, J. Niu, Electrochemically enhanced removal of perfluorinated compounds (PFCs) from aqueous solution by CNTs-graphene composite electrode, Chem. Eng. J. 328 (2017) 228–235.

[45] L. Ji, W. Chen, S. Zheng, Z. Xu, D. Zhu, Adsorption of sulfonamide antibiotics to multiwalled carbon nanotubes, Langmuir ACS J. Surf. Coll. 25 (2009) 11608.

[46] X. Zhou, S. Liu, A. Xu, K. Wei, W. Han, J. Li, X. Sun, J. Shen, X. Liu, L. Wang, A multi-walled carbon nanotube electrode based on porous Graphite-RuO2 in electrochemical filter for pyrrole degradation, Chem. Eng. J. 330 (2017) 956–964.

[47] H. Chen, B. Gao, H. Li, L.Q. Ma, Effects of pH and ionic strength on sulfamethoxazole and ciprofloxacin transport in saturated porous media, J. Contam. Hydrol. 126 (2011) 29–36.

[48] E.S. Elmolla, M. Chaudhuri, Degradation of amoxicillin, ampicillin and cloxacillin antibiotics in aqueous solution by the UV/ZnO photocatalytic process, J. Hazard. Mater. 173 (2010) 445–449.

[49] Y. Fan, Y. Ji, D. Kong, J. Lu, Q. Zhou, Kinetic and mechanistic investigations of the degradation of sulfamethazine in heat-activated persulfate oxidation process, J. Hazard. Mater. 300 (2015) 39–47.

[50] Y. Zhang, T. Yu, W. Han, X. Sun, J. Li, J. Shen, L. Wang, Electrochemical treatment of anticancer drugs wastewater containing 5-Fluoro-2-Methoxypyrimidine using a tubular porous electrode electrocatalytic reactor, Electrochim. Acta 220 (2016) 211–221.

[51] Y. Tian, B. Gao, K.J. Ziegler, High mobility of SDBS-dispersed single-walled carbon nanotubes in saturated and unsaturated porous media, J. Hazard. Mater. 186 (2011) 1766–1772.

[52] B. Song, P. Xu, G. Zeng, J. Gong, X. Wang, J. Yan, S. Wang, P. Zhang, W. Cao, S. Ye, Modeling the transport of sodium dodecyl benzene sulfonate in riverine sediment in the presence of multi-walled carbon nanotubes, Water Res. 129 (2018) 20–28.

[53] A. Deshpande, K. Baheti, N. Chatterjee, Degradation of β-lactam antibiotics, Curr. Sci. (2004) 1684–1695.

[54] A. Yada, S. Okajima, M. Murakami, Palladium-Catalyzed Intramolecular Insertion of Alkenes into the Carbon-Nitrogen Bond of β-Lactams, J. Am. Chem. Soc. 137 (2015) 8708–8711.

[55] Y. Ji, C. Ferronato, A. Salvador, X. Yang, J.-M. Chovelon, Degradation of ciprofloxacin and sulfamethoxazole by ferrous-activated persulfate: implications for remediation of groundwater contaminated by antibiotics, Sci. Total Environ. 472 (2014) 800–808.

[56] J. Yang, Z. Li, H. Zhu, Adsorption and photocatalytic degradation of sulfamethoxazole by a novel composite hydrogel with visible light irradiation, Appl. Catal. B 217 (2017) 603–614.

[57] Y. Wang, C. Shen, M. Zhang, B.-T. Zhang, Y.-G. Yu, The electrochemical degradation of ciprofloxacin using a SnO2-Sb/Ti anode: influencing factors, reaction pathways and energy demand, Chem. Eng. J. 296 (2016) 79–89.

[58] E. Ioannidou, Z. Frontistis, M. Antonopoulou, D. Venieri, I. Konstantinou, D.I. Kondarides, D. Mantzavinos, Solar photocatalytic degradation of sulfamethoxazole over tungsten – modified TiO 2, Chem. Eng. J. (2016).

[59] W.Q. Guo, R.L. Yin, X.J. Zhou, J.S. Du, H.O. Cao, S.S. Yang, N.Q. Ren, Sulfamethoxazole degradation by ultrasound/ozone oxidation process in water: kinetics, mechanisms, and pathways, Ultrason. Sonochem. 22 (2015) 182–187.

[60] Y. Ji, Y. Fan, K. Liu, D. Kong, J. Lu, Thermo activated persulfate oxidation of antibiotic sulfamethoxazole and structurally related compounds, Water Res. 87 (2015) 1–9.

[61] A.G. Trovó, R.F. Nogueira, A. Agüera, A.R. Fernandezalba, C. Sirtori, S. Malato, Degradation of sulfamethoxazole in water by solar photo-Fenton, Chem. Toxicol. Eval., Water Res. 43 (2009) 3922–3931.

[62] S.K. Mondal, A.K. Saha, A. Sinha, Removal of ciprofloxacin using modified advanced oxidation processes: kinetics, pathways and process optimization, J. Cleaner Prod. 171 (2018) 1203–1214.

[63] S. Li, J. Hu, Transformation products formation of ciprofloxacin in UVA/LED and UVA/LED/TiO 2 systems: Impact of natural organic matter characteristics, Water Res. 132 (2018) 320.

[64] T. An, H. Yang, G. Li, W. Song, W.J. Cooper, X. Nie, Kinetics and mechanism of advanced oxidation processes (AOPs) in degradation of ciprofloxacin in water, Appl. Catal. B 94 (2010) 288–294.

[65] W. Guo, Q.-L. Wu, X.-J. Zhou, H.-O. Cao, J.-S. Du, R.-L. Yin, N.-Q. Ren, Enhanced amoxicillin treatment using the electro-peroxone process: key factors and degradation mechanism, RSC Adv. 5 (2015) 52695–52702.

[66] D. Klauson, J. Babkina, K. Stepanova, M. Krichevskaya, S. Preis, Aqueous photocatalytic oxidation of amoxicillin, Catal. Today 151 (2010) 39–45.

[67] A.G. Trovó, R.F.P. Nogueira, A. Ana, A.R. Fernandez-Alba, M. Sixto, Degradation of the antibiotic amoxicillin by photo-Fenton process–chemical and toxicological assessment, Water Res. 45 (2011) 1394–1402.

[68] H. Liu, J. Liu, Y. Liu, K. Bertoldi, C.D. Vecitis, Quantitative 2D electrooxidative carbon nanotube filter model: Insight into reactive sites, Carbon 80 (2014) 651–664.